Journal of Drug Targeting

Original paper

One-step formation of lipid-polyacrylic acid-calcium carbonate nanoparticles for co-delivery of doxorubicin and curcumin

Jianqing Peng [a], Shintaro Fumoto [a,*], Hirotaka Miyamoto [a], Yi Chen [b], Naotaka Kuroda [a], Koyo Nishida [a]

[a] *Graduate School of Biomedical Sciences, Nagasaki University, Nagasaki 852-8501, Japan*

[b] *Department of pharmaceutics, China Pharmaceutical University, 24 Tongjiaxiang, Nanjing 210009, China*

*Corresponding author. E-mail address: sfumoto@nagasaki-u.ac.jp. Tel: 095-819-8568; fax: 095-819-8567

Abstract

A doxorubicin (Dox) and curcumin (Cur) combination treatment regimen has been widely studied in pre-clinical research. However, the nanoparticles developed for this combination therapy require a consecutive drug loading process because of the different water-solubility of these drugs. The present study provides a strategy for the 'one-step' formation of nanoparticles encapsulating both Dox and Cur. We took advantage of polyacrylic acid (PAA) and calcium carbonate ($CaCO_3$) to realise a high drug entrapment efficiency and pH-sensitive drug release using a simplified preparation method. Optimisation of lipid ratios and concentrations of $CaCO_3$ was conducted. Under optimal conditions, the mean diameter of PEGylated lipid/PAA/$CaCO_3$ nanoparticles with encapsulated Cur and Dox (LPCCD) was less than 100 nm. An obvious pH-sensitive release of both drugs was observed, with different Dox and Cur release rates. Successful co-delivery of Cur and Dox was achieved via LPCCD on HepG2 cells. LPCCD altered the bio-distribution of Dox and Cur *in vivo* and decreased Dox-induced cardiotoxicity. The current investigation has developed an efficient ternary system for co-delivery of Dox and Cur to tumours, using a 'one-step' formation resulting in nanoparticles possessing remarkable pH-sensitive drug release behaviour, which may be valuable for further clinical studies and eventual clinical application.

Keywords: doxorubicin, curcumin, polyacrylic acid, calcium carbonate, lipid nanoparticle

1. Introduction

In cancer treatment, combination therapy is widely applied in patients to achieve enhanced therapeutic efficacy and a reduction in side-effects. As a superior strategy to circumvent multi-drug resistant (MDR) effects, combination therapy is generally applied for advanced tumours (Misra and Sahoo, 2011, Huang *et al.*, 2015) and in terminal cancer patients (Jiang *et al.*, 2014). A large number of drug delivery systems (DDSs) have been developed, with the aim of achieving targeted drug delivery to tumour tissues and cells. However, conventional single drug DDSs cannot be used for combination therapy, especially for drug combinations including both lipophilic and hydrophilic drugs.

Previous studies have indicated that the combination of doxorubicin (Dox) and curcumin (Cur) is a promising combination therapy for cancer treatment (Misra and Sahoo, 2011, Duan *et al.*, 2012). Since the application of Dox is limited by cardiotoxicity and the emergence of the MDR effect. Cur, with a wide range of pharmacological effects, has been applied to overcome the MDR problem and ameliorate the side-effects (Duan *et al.*, 2012, Pramanik *et al.*, 2012). A variety of nano-carriers has been developed in expectation of improving the solubility of Cur and realising co-delivery of both Dox and Cur. Wang *et al*. developed Cur-Dox/MPEG-PCL micelles (Wang *et al.*, 2013). During their preparation, Cur and MPEG-PCL were first self-assembled into a core-shell structured Cur/MPEG-PCL micelle, and then Dox was encapsulated in a buffer (pH 7.4). Barui *et al.* encapsulated both Cur and Dox into a ligand-modified liposome using a film dispersion method and a pH gradient method, separately (Barui *et al.*, 2014). In such a DDS, a separated encapsulation procedure is inevitable because of the different levels of water solubility of the drugs. This complexity in preparation restricts the potential application of such a DDS. To this end, a nanoplatform exploiting a ‘one-step’ formation method for combination therapies is in need.

Calcium carbonate ($CaCO_3$) has been widely studied as a carrier or component of nanoparticles in order to facilitate the delivery of drugs and genes (Ueno *et al.*, 2005, Sharma *et al.*, 2015). In the presence of polyanion-DNA, $CaCO_3$ nanoparticles can be formed. The presence of $CaCO_3$ precipitation might control the size of DNA/$CaCO_3$ co-precipitation and enhance gene delivery (Zhao *et al.*, 2014). Moreover, the inherent pH-sensitivity of $CaCO_3$ might be useful to promote the dissociation of nanoparticles and endosome/lysosome escape under low pH conditions (Gong *et al.*, 2015, Min *et al.*,

2015). Considering the feasibility of $CaCO_3$ formation in the presence of Ca^{2+} and CO_3^{2-} ions, a promising strategy involves including $CaCO_3$ in a DDS as an inducer of drug release.

To increase the encapsulation of water soluble drug, Dox, a polyanion polyacrylic acid (PAA) was employed in this system. Previous studies have shown that PAA and Dox can form complexes with a pH-dependent interaction (Kitaeva *et al.*, 2004). Based on the results of a previous study, we chose a higher molecular weight PAA to achieve a high Dox encapsulation and a condensed structure for the PAA/Dox complexes.

In the current study, we designed a one-step formation method for a novel PEGylated lipid/PAA/$CaCO_3$ ternary system encapsulating Cur and Dox (LPCCD) aimed at increased tumour inhibitory effects and decreased cardiotoxicity. After formulation optimisation, the pH-sensitivity, cellular uptake, *in vitro* tumour suppression, *in vivo* bio-distribution and safety of the LPCCD nanoparticles were studied.

2. Materials and methods

2.1 Materials and reagents

Egg lecithin (EPC), Cur and PAA (Mw: 25 kDa) were purchased from Wako Pure Chemical Industries (Osaka, Japan). DSPE-020CN (*N*-(Carbonyl-methoxypolyethyleneglycol 2000)-1,2-distearoyl-sn-glycero-3-phosphoethanolamine, DSPE-PEG_{2000}) was obtained from NOF corporation (Tokyo, Japan) and 1,2-dioleoyl-3-trimethylammonium-propane (DOTAP) was obtained from Avanti Polar Lipids (Alabaster, AL, USA). Doxorubicin hydrochloride (Dox) was provided by Tokyo Chemical Industry Co., Ltd. (Tokyo, Japan). The other inorganic chemicals were obtained from Nacalai Tesque (Kyoto, Japan). All organic solvents of analytical grade were purchased from Sigma-Aldrich (St. Louis, MO, USA). Water used in all experiments was prepared through Direct-Q UV (Merck Millipore, Merck KGaA, Darmstadt, Germany.).

2.2 Cells and animals

HepG2 liver tumour cells were obtained from RIKEN (Tokyo, Japan). All cell culture media were purchased from Thermo Fisher Scientific (Waltham, MA USA).

Male ddY mice (25–27 g) and Wistar rats (230–280 g) supplied by Kyudo Co., Ltd. (Kumamoto, Japan) were fed a standard laboratory diet and were housed at an ambient temperature and humidity in air-conditioned chambers before the experiments. All

animal experiments were conducted in full compliance with the Guideline for Animal Experimentation at Nagasaki University.

2.3 Preparation and optimisation of nanoparticles

The ethanol injection method was used in the preparation of this ternary system. A 1 M $CaCl_2$ ethanol solution, a 3 mg/mL Cur ethanol solution and a 10 mg/mL Dox water solution were prepared as stock solutions. A certain amount of EPC, DOTAP and DSPE-PEG was dissolved in 8 mL of ethanol. Under stirring, a $CaCl_2$ solution, 1 mL of Cur solution and 0.5 mL of Dox solution were added dropwise to the lipid mixture solution in sequence and stirred for another 1 h at room temperature (ethanol phase). Meanwhile, a 5 mM Na_2CO_3 water solution including 1.25% glucose was prepared. After a certain amount of PAA was solubilised in 40 mL of the Na_2CO_3/glucose solution and stirred for another 1 h (water phase), the ethanol phase was added dropwise to the water phase with stirring for 2 h at room temperature. Then, the obtained mixture was maintained in a rotary evaporator (EYELA, Tokyo, Japan) under vacuum for 30 min at 40°C to evaporate the ethanol and concentrate the mixture to 10 mL. The obtained suspension was vortexed for 3 min and passed through a 0.8 μm filter to produce the LPCCD nanoparticles. In the preparation of a LPC blank carrier, the Cur and Dox solutions were not added, and the procedure was identical in all other respects.

In the optimisation of the formulation, the $CaCO_3$ concentration was varied and the ratio of PAA/DOTAP and DOTAP/EPC were studied. The diameter, polydispersity index (PDI), zeta potential and drug content of the nanoparticles were taken into consideration for the evaluation and confirmation of the optimised formulation.

2.4 Characterisation of LPC and LPCCD

The particle size, PDI and zeta potential of the LPC and LPCCD were assessed using a Zetasizer Nano ZS (Malvern, UK). To investigate the size variation of the lipid nanoparticles under different pH conditions, 0.01 M pH 7.4 Hepes buffer and 0.01 M pH 5.5 Mes buffer were used for the dilution of the nanoparticles at a ratio of 3:1 (v/v). Changes in the size distribution of the LPC and LPCCD were recorded after a 2 h incubation.

The drug content, drug loading capacity (DL) and entrapment efficiency (EE) of Dox and Cur were determined using high performance liquid chromatography (HPLC) with a UV detector (SPD-10A, Shimadzu, Kyoto, Japan). Briefly, 50 μL of the LPCCD

solution was added to 5 mL of a 1% Triton X-100 solution. The solution was sonicated for 1 min and centrifuged at 12,000 × *g* for 10 min (KUBOTA, Tokyo, Japan). The supernatant was analysed using a mobile phase of 5% acetic acid:acetonitrile = 60:40 (v/v) at λ = 420 nm to determine the Cur concentration in the LPCCD. For the measurement of Dox concentration, a mobile phase of 0.3% sodium dodecyl sulphate (adjusting pH to 2.7 using phosphoric acid):acetonitrile:methanol = 60:40:1 (v/v) at λ = 484 nm was used. The mobile phase was delivered at 1 mL/min through a C_{18} column (Cosmosil-Pak, 4.6 × 150 mm, internal diameter 5 μm). DL and EE were calculated in accordance with the following equations:

$$\mathrm{DL\,(wt.\%)} = \frac{\text{weight of loaded drug}}{\text{theoretical total weight of nanoparticles}} \times 100 \qquad (1)$$

$$\mathrm{EE\,(wt.\%)} = \frac{\text{weight of loaded drug}}{\text{weight of feeding drug}} \times 100 \qquad (2)$$

2.5 pH-sensitive drug release

Drug release behaviour was monitored using a membrane dialysis technique. 0.01 M pH 7.4 Hepes buffer (including 0.1% Tween 80) and 0.01M pH 5.5 Mes buffer (including 0.1% Tween 80) were prepared to simulate the physiological environment and lysosome/endosome microenvironment, respectively. A LPCCD solution (0.2 mL) was placed into a dialysis bag (molecular weight cutoff, 12 kDa) and exposed to 20 mL of pH 7.4 and pH 5.5 buffer. In addition, 0.2 mL of LPCCD solution with 10% foetal bovine serum (FBS; v/v) was also exposed to 20 mL of pH 7.4 buffer to determine the effect of FBS on the stability of LPCCD. In a shaking water bath, the drug release was determined for 30 h at 37°C. At certain intervals, 0.1 mL of medium was withdrawn and the same amount of fresh medium was replenished. The concentration of Dox and Cur was determined using HPLC.

2.6 Haemolysis activity

Fresh rat arterial blood was centrifuged at 1630 × *g* for 10 min in pH 7.4 phosphate-buffered saline (PBS) to collect the red blood cells (RBCs). This step was repeated three times and the RBCs were resuspended in PBS. LPC and the liposome (prepared using the same amount of EPC, DOTAP and DSPE-PEG with the ethanol injection method) at various concentrations of lipids were incubated with a 10 % (v/v) RBC suspension at a ratio of 1:4 (v/v) and shaken in a water bath at 37°C for 1 h. Milli-Q water and PBS

were incubated with the RBC suspension using the same procedure, as a positive and negative control, respectively. After a 1 h incubation, the mixture was centrifuged at 1,630 × *g* for 10 min and the supernatant was analysed using a spectrophotometer (UV-1600, Shimadzu, Kyoto, Japan) at λ = 550 nm. The haemolysis percentage was calculated using the following equation:

$$\text{Haemolysis}\,(\%) = \frac{\text{absorbance of sample} - \text{absorbance of negative control}}{\text{absorbance of positive control} - \text{absorbance of negative control}} \times 100 \quad (3)$$

2.7 In vitro cellular uptake

HepG2 cells were cultured in Dulbecco's modified Eagle medium (DMEM) including 10% FBS and 10,000 U/mL of penicillin/streptomycin at 37°C, 5% CO_2 and 90% relative humidity. For the cellular uptake evaluation, the cells were seeded at a density of 1×10^5 cells/well in six-well plates. After a 12 h incubation, the cells were incubated with free Dox, Dox + Cur (1:1, mol/mol) and LPCCD (final concentration of 5 μM of Dox) in FBS-free medium for a certain period of time at 37°C. Then, the supernatant was removed and the cells were washed using PBS (pH 7.4) three times. The cells were fixed in 4% paraformaldehyde for 15 min and washed using PBS again. After two drops of Slow Fade Diamond® (Thermo Fisher Scientific) were added, the samples were observed using confocal microscopy (Carl Zeiss Microimaging GmbH, Jena, Germany). To quantify the DOX cellular uptake, a fluorescence-activated cell-sorting flow cytometer (Beckman Coulter, Brea, CA, USA) was employed. After incubation with the samples for 4 h, the supernatant was removed. The cells were washed with PBS and trypsinised, in accordance with a standard protocol. After resuspension of the cells in 0.5 mL of PBS, the mean fluorescence intensity of the Dox was detected.

2.8 In vitro cytotoxicity

For an evaluation of cytotoxicity, the cells were seeded in 96-well plates at a density of 1×10^4 cells/well. Dox, Dox + Cur (1:1, mol/mol), LPC and LPCCD at various concentrations were added to the wells after a 12 h incubation. The cells were further incubated for 48 h, the medium was removed and the cells were washed with PBS. DMEM (100 μL) including 10 μL of cell counting kit-8 (Dojindo, Kumamoto, Japan) was added to each well and incubated for 1 h. The absorbance was measured at 450 nm using a microplate photometer (Multiskan™ FC, Thermo Fisher Scientific). Blank wells and untreated cells served as a negative control and positive control, respectively.

2.9 Bio-distribution of the nanoparticles

A free Dox + Cur solution and LPCCD (at an equivalent Dox concentration of 0.4 mg/mL and Cur at 0.24 mg/mL) were intravenously injected in ddY mice at a Dox dose of 3 mg/kg. Mice were anesthetised using a drug mix (butorphanol, medetomidine and midazolam) 3 h after the treatment injection. Blood was taken from the inferior vena cava, and the heart, liver, spleen, lung and kidney were harvested and weighed. Dox and Cur were extracted as reported in a previous study (Abdalkader *et al.*, 2015). Briefly, organs were homogenised using a mixed solution of isopropanol and 1 M HCl (1:1, v/v) and incubated at 4°C for 1 h. The solutions were centrifuged at 1,630 × *g* for 15 min, and the supernatants were centrifuged again at 15,000 × *g* for 15 min. In the case of determining the drug concentration in plasma, the blood was centrifuged at 1,500 × *g* for 10 min. The plasma supernatant was mixed with an isopropanol:1 M HCl = 1:1 (v/v) mixture and acetonitrile for the detection of Dox and Cur. The supernatants were analysed using a fluorescence spectrometer (RF-5300PC, Shimadzu, Kyoto, Japan). For the detection of Dox, the excitation (Ex) and emission (Em) wavelength was 500 and 590 nm, respectively. An Ex/Em of 440/500 nm was used in the detection of Cur. Standard curves of Dox and Cur were prepared using blank organ extracts.

2.10 Histopathological analysis of cardiotoxicity

Free Dox and LPCCD were injected intravenously in ddY mice at a 5 mg/kg Dox equivalent once daily for 3 days. Six hours following the last injection, a histopathological analysis was performed on the heart. Briefly, after tissue perfusion, the heart was harvested and fixed using 4% paraformaldehyde, immersed in sucrose solution and embedded in O.C.T compound. The frozen tissues were sliced at a 5 μm thickness and stained using haematoxylin and eosin (H&E). A morphological evaluation was performed using a microscope (Carl Zeiss, Jena, Germany).

2.11 Statistical analysis

The data are presented as mean ± standard deviations (SD) of at least three independent experiments. Significant differences were identified using Student's *t*-test and one-way ANOVA analysis followed by Bonferroni's post hoc test. A *P*-value of less than 0.05 was considered to be statistically significant.

3. Results

3.1 Optimisation of the LPCCD

'One-step' formation of nanoparticles with encapsulated Dox and Cur was achieved using the ethanol injection method. The concentration of $CaCO_3$, and the PAA/DOTAP and EPC/DOTAP weight ratios were optimised based on the characteristics of the nanoparticles and the loaded drug content.

The diameter of the nanoparticles prepared using various concentrations of $CaCO_3$ was approximately 100 nm (**Fig. 1**). As the concentration of $CaCO_3$ increased, a charge reversal was observed in the zeta potential. At 20 mM of $CaCO_3$, both Cur and Dox exhibited the highest level of encapsulation. Given that the smallest diameter and PDI were detected at 20 mM of $CaCO_3$, this concentration of $CaCO_3$ was used in the following experiments.

In terms of the PAA/DOTAP weight ratio (**Fig. 2**), the diameter of both the LPC and the LPCCD was less than 100 nm, except for the LPCCD prepared at 16:5, while poor mono-dispersity was shown at a low weight ratio (4:5). Charge reversal was observed on the addition of PAA. The charge potential of the nanoparticles decreased after Dox encapsulation. The highest dox encapsulation was achieved at a PAA/DOTAP weight ratio of 8:5. Moreover, increased PAA restricted the encapsulation of Cur. Therefore, at a PAA/DOTAP weight ratio of 8:5, the balance in nanoparticle size, PDI and drug content was the best.

Next, we optimised the EPC/DOTAP weight ratio (**Fig. 3**). Nanoparticles less than 100 nm in diameter were achieved at an EPC/DOTAP weight ratio of 4:1. The PDI had a tendency to increase at higher ratios of EPC/DOTAP. Cur encapsulation was the best at an EPC/DOTAP weight ratio of 4:1. As the EPC/DOTAP weight ratio increased to 6:1, Dox encapsulation was greatly decreased. Therefore, taking the characteristics of the nanoparticles and the drug loading data into consideration, the LPCCD prepared at an EPC/DOTAP weight ratio of 4:1 were optimal.

3.2 Characterisation of the LPC and LPCCD

Under the optimised conditions, the diameters of both LPC and LPCCD were less than 100 nm with a reasonable mono-dispersity (**Table. 1**). The entrapment efficiency of both Dox and Cur was higher than 80% showing a molar ratio of Dox/Cur of approximately 1:1 (**Table. 2**). Next, we measured the UV spectrum of Dox and Cur in the LPCCD (**Fig. 4**). It was clear that the characteristic peak of Cur around 430 nm overlapped with that of the LPCCD. However, one of the Dox characteristic peaks

around 250 nm shifted to the left side of the curve of the LPCCD and the other Dox peaks around 500 nm decreased.

3.3 pH-sensitivity and stability of the nanoparticles

DDSs with pH-sensitivity are promising for efficient intracellular drug release. The variation of the particle size distributions of both LPC and LPCCD when mixed with buffer solutions at different pH values might indicate a morphological change in the nanoparticles (**Supplementary Fig. 1**). In particular, in the LPCCD sample, the curve at pH 5.5 shifted slightly to the right and the intensity decreased.

The drug release behaviour at different pH values was also studied. Both Dox and Cur release exhibited a noticeable sensitivity to pH, which was particularly pronounced for Dox release (**Fig. 5A**). As the pH decreased from 7.4 (physiological conditions) to 5.5 (lysosome/endosome environment), a sharply increased release of Dox was observed. However, Cur showed a delayed release at pH 5.5 compared with Dox. In addition, the release behaviour of both Dox and Cur in the presence of 10% FBS was indistinguishable from that in the samples without FBS (**Fig. 5B**).

3.4 Evaluation of the cellular uptake of the LPCCD

Both Dox and Cur possess fluorescence that that can be used to indicate their intracellular distribution. Using microscopy, Dox was clearly observed to enter the nucleus in the free drug groups, while the fluorescence of Cur was undetectable (**Fig. 6**). In the case of the LPCCD groups, the cellular uptake of both of Dox and Cur increased along with time until 8 h, at which apoptosis may have occurred as indicated by nuclear perforations. The released Dox overlapped with Cur, which is indicated by a yellow colour. It was clear that LPCCD enhanced the cellular uptake of Cur into the cytoplasm and the increased accumulation of Dox in the nucleus might have resulted from pH-sensitive drug release. However, the cellular uptake and nuclear penetration of Dox in the LPCCD groups was not as good as in the free drug groups. The quantitation of cellular uptake was conducted using a flow cytometer, and it was demonstrated that the mean fluorescence intensity of cells treated using LPCCD was approximately half that of the free drug groups (**Fig. 7**).

3.5 Cytotoxicity and safety of the nanoparticles

An *in vitro* cell-growth inhibition study was performed using HepG2 cells (**Fig. 8**). At a low concentration of Dox, the inhibitory effect of the free Dox and LPCCD on cell growth was slightly inferior to that of the free drug combination. As the drug concentration increased, LPCCD exhibited higher cytotoxicity compared with Dox and Dox + Cur groups (**Fig. 8A**). The IC_{50} of Dox, Dox + Cur and the LPCCD was 0.1645, 0.0491 and 0.1256 μM, respectively. The LPC blank carrier produced no inhibitory effects on the growth of tumour cells at corresponding concentrations of EPC (**Fig. 8B**). Meanwhile, significant levels of haemolysis were not produced by either the LPC or liposomes prepared without PAA and $CaCO_3$ (**Supplementary Fig. 2**). Even at the highest concentration of total lipid, the haemolysis was below 5% and the nanoparticles were deemed to possess no haemolytic activity *in vitro*. Importantly, the $CaCO_3$ was verified to not produce a burst release of Ca^{2+} ions under physiological conditions, which might affect the stability of erythrocytes. Therefore, the nanoparticles were suitable for an *in vivo* study.

3.6 Bio-distribution of Dox in mice

We checked the prolonged blood circulation of LPCCD in ddY mice (**Fig. 9**). LPCCD significantly increased the blood concentration of Dox and Cur at 3 h as compared with the free drugs groups (**Fig. 9A and D**). The accumulation of Dox and Cur in the spleen from delivered LPCCD was significantly increased compared with the free drugs groups (**Fig. 9B and E**). In the liver, lung and kidney, both Dox and Cur showed decreased distribution. Meanwhile, an obviously reduced distribution of Dox to the heart from the delivered LPCCD was observed related to the free Dox group. Distribution patterns of Dox and Cur in LPCCD group indicated apparently different accumulations between Dox and Cur, especially in the spleen and lung. This implied that a part of LPCCD were broken during blood circulation and subsequently released Dox and Cur partitioned from blood to tissues. As clearly shown from the obtained tissue/plasma ratios, nanoparticle formulation greatly decreased the partition of Dox and Cur from plasma to tissue (**Fig. 9C and F**). It is reasonable to conclude that the LPCCD avoid the fast clearance of drugs in circulation and alter the bio-distribution of Dox and Cur *in vivo*.

3.7 Evaluation of the cardiotoxicity induced by Dox

A histological assay was performed on heart cryosections to evaluate Dox-induced cardiotoxicity. The morphology of the tissue was observed using light microscopy after

a H&E stain on cross-sections of the cardiac tissue (**Fig. 10**). Normal tissue morphology was observed in the saline group. A number of cells with significant oedema are indicated using black arrows in the free Dox-treated group, indicating inflammation after continuous doses. In addition, hypertrophic cardiac cells, identified from their elongated nuclei, were revealed in the free Dox-treated group (white arrows). In contrast, no inflammatory cells or hypertrophic cardiac cells were observed in the LPCCD group at an equivalent dose of Dox.

4. Discussion

Combination therapy, with its obvious advantages, has been generally employed as a therapeutic regimen for cancer treatments. The sole use of Dox, a widely used chemotherapeutic drug in clinical treatment, is associated with the development of MDR and cardiotoxicity problems. Preclinical research has shown that combining Dox with Cur, which possesses promising pharmacological effects, can overcome the setbacks of using Dox alone (Sadzuka *et al.*, 2012). A significant amount of research has been dedicated to harnessing the synergistic effects of this combination therapy in tumour inhibition. Micelles, nanocapsules and liposomes with functional components have been developed to achieve efficient co-delivery of Dox and Cur (Barui *et al.*, 2014, Fang *et al.*, 2014, Li *et al.*, 2015). However, multi-step methods for nanoparticle preparation and drug encapsulation were involved. Therefore, we have developed a simplified method for the simultaneous encapsulation of Dox and Cur within ‘one step’, resulting in the LPCCD nanoparticles. The key point for the ‘one-step’ formation of the LPCCD was utilisation of the phenomenon that $CaCl_2$ is soluble in ethanol. Addition of $CaCl_2$ into the ethanol phase with other components including lipids, Dox, and Cur enabled us to form lipid/polyanion/$CaCO_3$ ternary nanoparticles containing drugs using an ethanol injection method. Therefore, the formation of highly organised LPCCD was successfully achieved within ‘one step’.

It has been previously reported that the complexation of PAA/Dox resulted in nanoparticles with a diameter ranging from 600 to 900 nm that possessed a pH dependent interaction, and smaller nanoparticles of approximately 200 nm were obtained after mixing them with liposomes (Kitaeva *et al.*, 2004). Enlightened by this study, we involved the PAA/Dox unit in the LPCCD system. In terms of Cur encapsulation, liposomes are a good choice. Therefore, the LPCCD co-delivery system was developed based on the triple complexation of lipid/Cur, PAA/Dox and $CaCO_3$. To

decrease the particle size of the nanoparticles and improve the Dox loading, a high molecular weight PAA (25 kDa) was utilised. Given that interaction between PAA/Dox complexes and lipids would affect the stability of the lipid bilayer and mono-dispersity of the final ternary system, a 'one-step' formation method with both encapsulated Dox and Cur was developed and optimised. Importantly, the use of a certain amount of the DOTAP positive lipid instead of the EPC neutral lipid was the key factor in achieving a successful 'one-step' formation.

During the optimisation of the formation conditions of the LPCCD, the concentration of $CaCO_3$, and the PAA/DOTAP and EPC/DOTAP weight ratios were important factors in determining the particle size, PDI, and drug content (**Figs. 1-3**). Increasing the concentration of $CaCO_3$ during the formation of the LPCCD caused the surface charge to change from negative to positive (**Fig. 1C**). This might be caused by the charge neutralisation of PAA by the Ca^{2+} ion. The Cur content decreased at 10 mM $CaCO_3$. A strong electrostatic interaction between polyanion PAA and the lipid bilayer containing the DOTAP cationic lipid might interfere with the insertion of Cur. A particular concentration of the Ca^{2+} ion was required for efficient drug loading of Cur. However, too high of a concentration of $CaCO_3$ might inhibit the stable formation of the nanoparticles. In fact, a 30 mM $CaCO_3$ concentration resulted in an increase in the PDI (**Fig. 1B**) and flocculation (data not shown). A reduced encapsulation of Dox in the LPCCD at a 30 mM $CaCO_3$ concentration was observed, possibly because of the filtration through filter. The electrostatic interactions between PAA and DOTAP played an important role in the formation of the nanoparticles (**Fig. 2**). Increasing the PAA/DOTAP ratio decreased the zeta potential, indicating that the surface of the nanoparticles was covered with PAA possessing carboxyl groups. Because Dox incorporation into the nanoparticles unexpectedly decreased the zeta potential, despite the cationic charge of Dox, the interaction between PAA and Dox may have inhibited the penetration of the PAA/$CaCO_3$/Dox complexes into the core of the lipid nanoparticles, resulting in a partial shift of PAA to the surface of the nanoparticles. Drug encapsulation was closely related to the PAA/DOTAP ratio. Charge balance and electrostatic interaction among PAA, DOTAP and Dox are important for the encapsulation of Dox. Increasing the PAA ratio decreased Cur encapsulation because of the interaction with DOTAP. There is no doubt that the lipid component proportions (EPC/DOTAP ratio) are closely related with the characteristics of the nanoparticles (**Fig. 3**). An increased amount of total lipid and the proportion of EPC increased the difficulty

in the formation of the nanoparticles, especially via a 'one-step' formation method. The increased weight ratio of EPC/DOTAP gave rise to a decreased positive charge density of the LPC. Both sharply reduced encapsulation of Dox and the increased PDI might be caused by the loss of LPCCD with a large size via passing through the filter. In general, strong negative and positive surface charge stabilise nanoparticles. This is in consistent with the properties of the LPCCD, since the particle size and PDI tended to be smaller when the zeta potential of the nanoparticles was approximately neutral (**Figs 1–3**). The formulation of LPCCD is complicated that contains several cations and anions. As cations, Dox, DOTAP and Ca^{2+} ions would interact with anion PAA and the CO_3^{2-} ion. If we assume that nanoparticle intermediates are present, the strong negative and positive charge of the intermediates undergo charge neutralisation from free cations and anions, respectively, and as a consequence the intermediates become large. The optimal concentration of $CaCO_3$, and the optimal PAA/DOTAP and EPC/DOTAP weight ratios were 20 mM, 8:5, and 4:1, respectively.

Under optimal conditions, the particle size of the nanoparticles was less than 100 nm, indicating their successful preparation (**Table 1**). The nanoparticles contained a sufficient amount of Dox and Cur (**Table 2**). The entrapment efficiencies for Dox and Cur were very high (**Table 2**). The encapsulation of Dox and Cur in the LPCCD was verified by recording their UV spectrum (**Fig. 4**). The characteristic Dox peak around 500 nm decreased, whereas the peak around 250 nm shifted to the left. This might be caused by a difference in the ionisation condition of Dox through neutralisation with PAA and the CO_3^{2-} ion. Under an acidic environment, the disruption of $CaCO_3$ and the dissociation of the Dox/PAA/$CaCO_3$ complexes would occur. Therefore, a change in pH might influence the stability of the LPCCD (**Supplementary Fig. 1**). Consistent with the size variation, both dissociation of the PAA/Dox complexes and the destruction of the $CaCO_3$ enhanced the drug release (**Fig. 5A**). In addition, the increased free Ca^{2+} ions might contribute to the enhanced Dox release by competitively inhibiting interaction with PAA. In the case of Cur, the dissociated PAA might combine with DOTAP to affect the stability of the lipid bilayer leading to a retarded release of Cur. Since the drug release was similar in 10% FBS (**Fig. 5B**), it is rational to suppose that the LPCCD can remain stable in *in vivo* circulation.

In the development of liposomes, pH-sensitive drug release has been pursued because of the stability of liposomes leading to a slow and incomplete drug release. Encapsulation of calcium phosphate and calcium carbonate during the formation of liposomes and

nanoparticles has resulted in an impressive pH-sensitivity and enhanced drug delivery (Li *et al.*, 2010, Li *et al.*, 2012). In the lysosome/endosome, low pH promotes an increase of calcium and bicarbonate/carbonate ions, the resulted osmotic swelling leading to a fast release of drugs into the cytoplasm (Kim *et al.*, 2013). To date, the delivery of DNA via liposomes in the presence of calcium phosphate and calcium carbonate was particularly intriguing in view of enhancing transfection efficiency (Hu *et al.*, 2013, Zhao *et al.*, 2014). The structural similarity between PAA and DNA in terms of the presence of large amounts of anion groups means that the co-precipitation of Ca^{2+}, Dox and PAA with CO_3^{2-} in the presence of the phospholipid might result in pH-sensitive in drug release. In the current study, the optimisation of the formulation clearly showed that the ratio between PAA, lipid and $CaCO_3$ was closely related with the characteristics of the formed nanoparticles and the drug loading efficiency (**Figs. 1–3**). An obvious pH-sensitive drug release was observed for both Dox and Cur (**Fig. 5A**). Not only the pH sensitivity of the combination between PAA and Dox, but also the destruction of $CaCO_3$ under an acidic environment might promote the burst release of Dox. Simultaneously, because of the existence of an electrostatic interaction between PAA and DOTAP, disruption of the PAA/Dox/$CaCO_3$ complexes at pH 5.5 resulted in instability in the lipid bilayer promoting a delayed release of Cur.

To guarantee the stability and mono-dispersity of the LPCCD nanoparticles, a certain amount of DSPE-PEG was necessary to prevent aggregation during the 'one-step' formation that involved complex electrostatic interactions between multiple components. The peripheral PEG moieties imparted stability to the LPCCD in the presence of FBS (**Fig. 5B**) and safety in terms of haemolysis (**Supplementary Fig. 2**). In addition, the blood circulation of the LPCCD was also greatly prolonged by the PEG coating by preventing phagocytosis by the immune cells of the reticuloendothelial system (**Fig. 9**). However, DSPE-PEG is a double-edged sword. A high ratio of DSPE-PEG in a lipid bilayer might suppress the cellular uptake of LPCCD, as potentially indicated by the reduced nuclear penetration of Dox (**Figs. 6–7**). The cytotoxicity of LPCCD on tumour cells was slightly inferior to the free drug combination group, despite a significantly reduced cellular uptake of Dox. However, taking the increased cellular uptake of Cur from the LPCCD into consideration, it is reasonable to conclude that the LPCCD promoted the antitumor effects of Dox and Cur via efficient co-delivery. For future tumour-selective delivery of LPCCD, the incorporation of tumour-specific ligands would be required.

The realisation of the synergistic effects of combination therapies relies on the efficient co-delivery of drugs to targeted organs. Generally, the *in vivo* bio-distribution behaviour of drugs is diverse because of the different metabolic pathways involved. With the employment of nanoparticles, the component drugs are capable to achieve desired spatiotemporal distribution *in vivo*. As shown in **Fig. 9**, the altered accumulation of both Dox and Cur in organs from the LPCCD compared with the free drugs group was observed in the *in vivo* distribution study. The increased plasma concentration and similar bio-distribution of the Dox and Cur *in vivo* from the LPCCD nanoparticles compared with the free drugs group provide a foundation for the realisation of enhanced synergistic effect of the combination therapy. In addition, the decreased distribution of Dox to the heart in the LPCCD group was consistent with the results from the histological assay of ameliorated cardiotoxicity (**Fig. 10**). Therefore, it is reasonable to hypothesise that co-delivery of Dox and Cur using LPCCD would be an effective delivery system with high safety.

5. Conclusions

We have successfully developed a $CaCO_3$-encapsulated PAA-stabilised lipid ternary system for Dox and Cur combination therapy. With the use of polyanion-PAA and $CaCO_3$, the LPCCD co-delivery system was achieved using a 'one-step' formation method and it possesses a robust pH-sensitive drug release. A narrow size distribution of nanoparticles of approximately 100 nm in diameter was achieved. The entrapment efficiencies of Dox and Cur in the LPCCD were high. Moreover, the LPCCD produced significant cytotoxicity in tumour cells and decreased cardiotoxicity compared with free Dox. In summary, the LPCCD nanoparticles have potential in cancer therapy and this ternary system is promising for further application with other chemotherapeutic combination therapies.

Acknowledgements

This work was supported in part by the Grants-in-Aid for Scientific Research from the Japan Society for the Promotion of Science.

Disclosure of interest

The authors report no conflicts of interest.

References

Abdalkader, R., Kawakami, S., Unga, J., Suzuki, R., Maruyama, K., Yamashita, F. & Hashida, M., 2015. Evaluation of the potential of doxorubicin loaded microbubbles as a theranostic modality using a murine tumour model. *Acta Biomater,* 19**,** 112-118.

Barui, S., Saha, S., Mondal, G., Haseena, S. & Chaudhuri, A., 2014. Simultaneous delivery of doxorubicin and curcumin encapsulated in liposomes of pegylated RGDK-lipopeptide to tumour vasculature. *Biomaterials,* 35**,** 1643-1656.

Duan, J., Mansour, H.M., Zhang, Y., Deng, X., Chen, Y., Wang, J., Pan, Y. & Zhao, J., 2012. Reversion of multidrug resistance by co-encapsulation of doxorubicin and curcumin in chitosan/poly (butyl cyanoacrylate) nanoparticles. *Int J Pharm,* 426**,** 193-201.

Fang, J.H., Lai, Y.H., Chiu, T.L., Chen, Y.Y., Hu, S.H. & Chen, S.Y., 2014. Magnetic core–shell nanocapsules with dual-targeting capabilities and co-delivery of multiple drugs to treat brain gliomas. *Adv Healthc Mater,* 3**,** 1250-1260.

Gong, M.-Q., Wu, J.-L., Chen, B., Zhuo, R.-X. & Cheng, S.-X., 2015. Self-assembled polymer/inorganic hybrid nanovesicles for multiple drug delivery to overcome drug resistance in cancer chemotherapy. *Langmuir,* 31**,** 5115-5122.

Hu, Y., Haynes, M.T., Wang, Y., Liu, F. & Huang, L., 2013. A highly efficient synthetic vector: nonhydrodynamic delivery of DNA to hepatocyte nuclei *in vivo*. *ACS Nano,* 7**,** 5376-5384.

Huang, W., Wu, Q.-D., Zhang, M., Kong, Y.-L., Cao, P.-R., Zheng, W., Xu, J.-H. & Ye, M., 2015. Novel Hsp90 inhibitor FW-04-806 displays potent antitumour effects in HER2-positive breast cancer cells as a single agent or in combination with lapatinib. *Cancer Lett,* 356**,** 862-871.

Jiang, H., Xu, L., Liu, D., Liu, K., Chen, S., Jiang, B., Jiang, Q., Chen, H., Chen, Y. & Han, W., 2014. Allogeneic hematopoietic SCT in combination with tyrosine kinase inhibitor treatment compared with TKI treatment alone in CML blast crisis. *Bone Marrow Transplant,* 49**,** 1146-1154.

Kim, S.K., Foote, M.B. & Huang, L., 2013. Targeted delivery of EV peptide to tumour cell cytoplasm using lipid coated calcium carbonate nanoparticles. *Cancer Lett,* 334**,** 311-318.

Kitaeva, M., Melik-Nubarov, N., Menger, F. & Yaroslavov, A., 2004. Doxorubicin-poly (acrylic acid) complexes: interaction with liposomes. *Langmuir,* 20**,** 6575-6579.

Li, H., Li, M., Chen, C., Fan, A., Kong, D., Wang, Z. & Zhao, Y., 2015. On-demand combinational delivery of curcumin and doxorubicin via a pH-labile micellar nanocarrier. *Int J Pharm,* 495**,** 572-578.

Li, J., Chen, Y.-C., Tseng, Y.-C., Mozumdar, S. & Huang, L., 2010. Biodegradable calcium phosphate nanoparticle with lipid coating for systemic siRNA delivery. *J Control Release,* 142**,** 416-421.

Li, J., Yang, Y. & Huang, L., 2012. Calcium phosphate nanoparticles with an asymmetric lipid bilayer coating for siRNA delivery to the tumour. *J Control Release,* 158**,** 108-114.

Min, K.H., Min, H.S., Lee, H.J., Park, D.J., Yhee, J.Y., Kim, K., Kwon, I.C., Jeong, S.Y., Silvestre, O.F. & Chen, X., 2015. pH-controlled gas-generating mineralized nanoparticles: a theranostic agent for ultrasound imaging and therapy of cancers. *ACS Nano,* 9**,** 134-145.

Misra, R. & Sahoo, S.K., 2011. Coformulation of doxorubicin and curcumin in poly (D, L-lactide-co-glycolide) nanoparticles suppresses the development of multidrug resistance in K562 cells. *Mol Pharm,* 8**,** 852-866.

Pramanik, D., Campbell, N.R., Das, S., Gupta, S., Chenna, V., Bisht, S., Sysa-Shah, P., Bedja, D., Karikari, C. & Steenbergen, C., 2012. A composite polymer nanoparticle overcomes multidrug resistance and ameliorates doxorubicin-associated cardiomyopathy. *Oncotarget,* 3**,** 640-650.

Sadzuka, Y., Nagamine, M., Toyooka, T., Ibuki, Y. & Sonobe, T., 2012. Beneficial effects of curcumin on antitumour activity and adverse reactions of doxorubicin. *Int J Pharm,* 432**,** 42-49.

Sharma, S., Verma, A., Teja, B.V., Pandey, G., Mittapelly, N., Trivedi, R. & Mishra, P., 2015. An insight into functionalized calcium based inorganic nanomaterials in biomedicine: Trends and transitions. *Colloids Surf B Biointerfaces,* 133**,** 120-139.

Ueno, Y., Futagawa, H., Takagi, Y., Ueno, A. & Mizushima, Y., 2005. Drug-incorporating calcium carbonate nanoparticles for a new delivery system. *J Control Release,* 103**,** 93-98.

Wang, B.-L., Shen, Y.-M., Zhang, Q.-W., Li, Y.-L., Luo, M., Liu, Z., Li, Y., Qian, Z.-Y., Gao, X. & Shi, H.-S., 2013. Codelivery of curcumin and doxorubicin by MPEG-PCL results in improved efficacy of systemically administered chemotherapy in mice with lung cancer. *Int J Nanomedicine,* 8**,** 3521.

Zhao, D., Wang, C.-Q., Zhuo, R.-X. & Cheng, S.-X., 2014. Modification of nanostructured calcium carbonate for efficient gene delivery. *Colloids Surf B Biointerfaces,* 118**,** 111-116.

Table 1. Diameter, PDI and zeta potential of LPCs and LPCCDs

Group	Diameter (nm)	PDI	Zeta potential (mV)
LPC	91.73 ± 1.15	0.140 ± 0.005	-2.07 ± 0.46
LPCCD	99.17 ± 0.31	0.189 ± 0.003	-2.82 ± 0.28

Table 2. Drug content, drug loading (DL) and entrapment efficiency (EE) of LPCCDs

Drug	Content (mg/mL)	DL(%)	EE(%)
Dox	0.405 ± 0.022	2.59 ± 0.14	80.95 ± 4.33
Cur	0.244 ± 0.008	1.58 ± 0.05	81.37 ± 2.64

List of figures

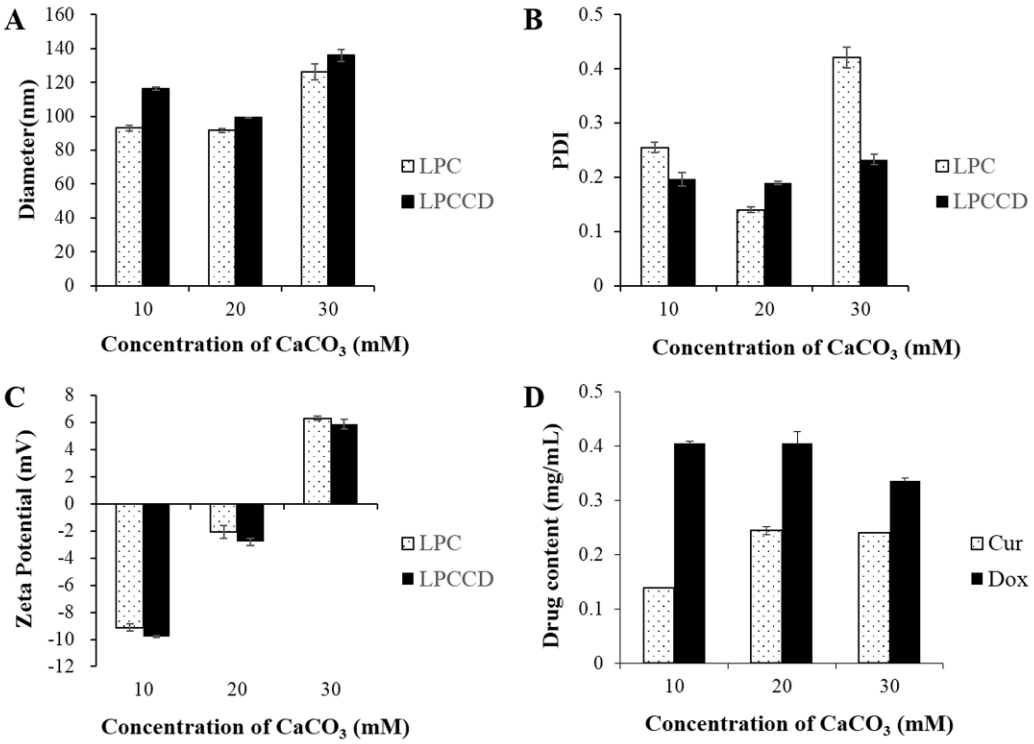

Fig. 1 The (A) diameter, (B) polydispersity index and (C) zeta potential of LPCCD and LPC and (D) Cur and Dox drug content in LPCCD with variation of the concentration of $CaCO_3$. Each bar represents the mean ± SD of three experiments.

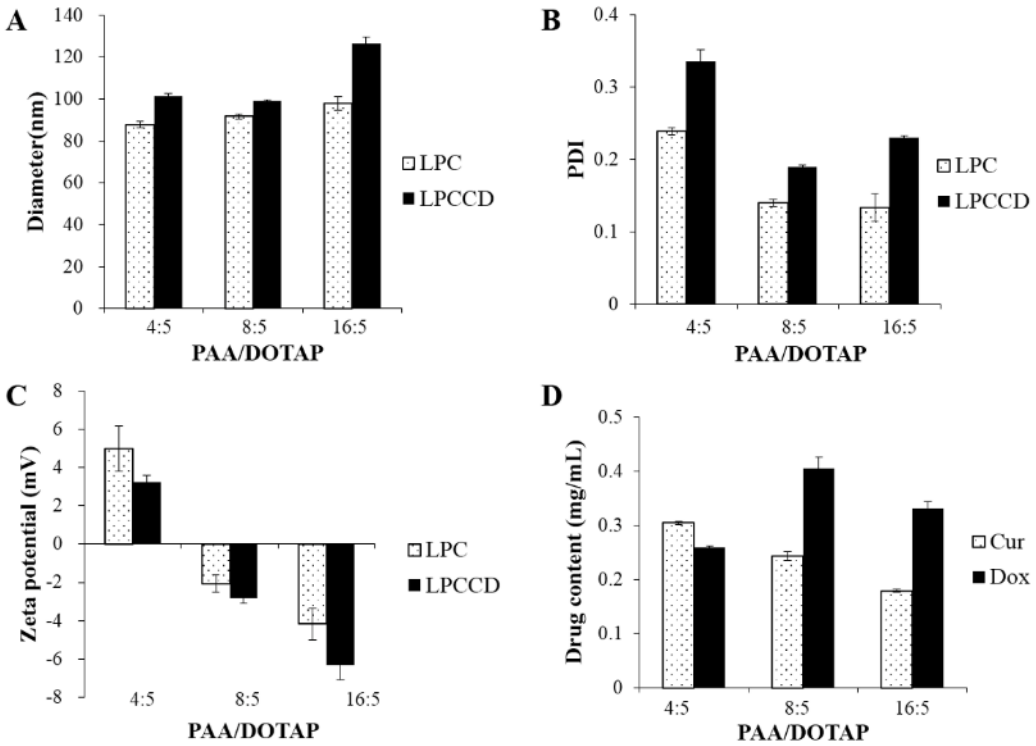

Fig. 2 The (A) diameter, (B) polydispersity index and (C) zeta potential of LPCCD and LPC and (D) Cur and Dox drug content in LPCCD with varied PAA/DOTAP weight ratios. Each bar represents the mean ± SD of three experiments.

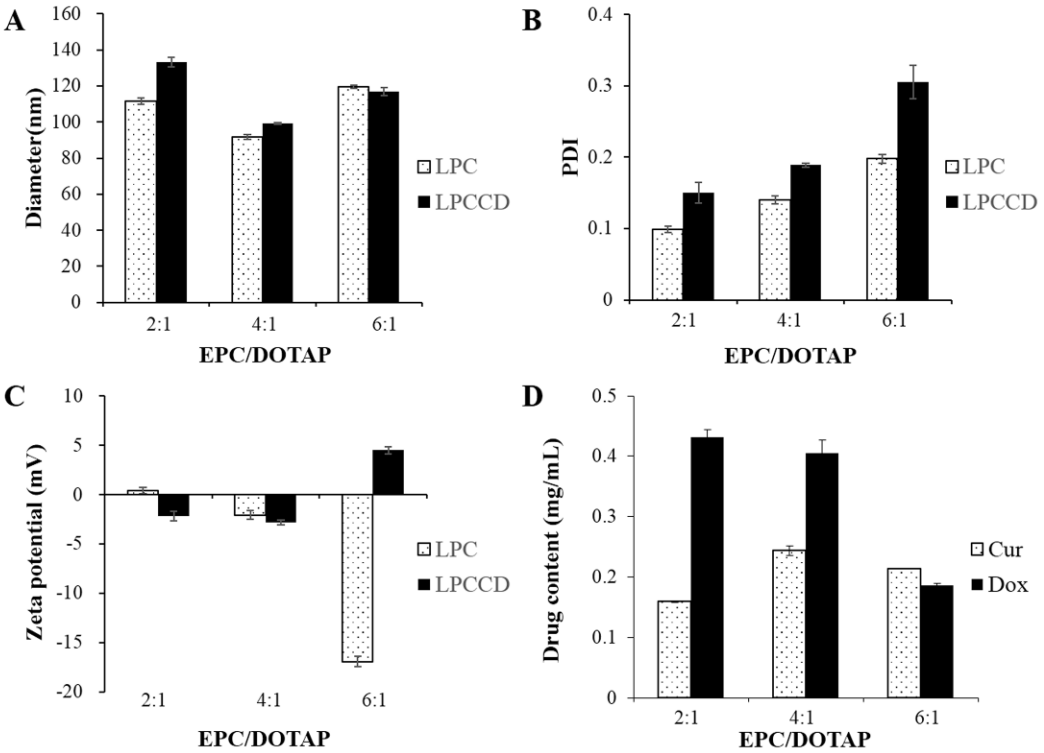

Fig. 3 The (A) diameter, (B) polydispersity index and (C) zeta potential of LPCCD and LPC and (D) Cur and Dox drug content in LPCCD with varied EPC/DOTAP weight ratios. Each bar represents the mean ± SD of three experiments.

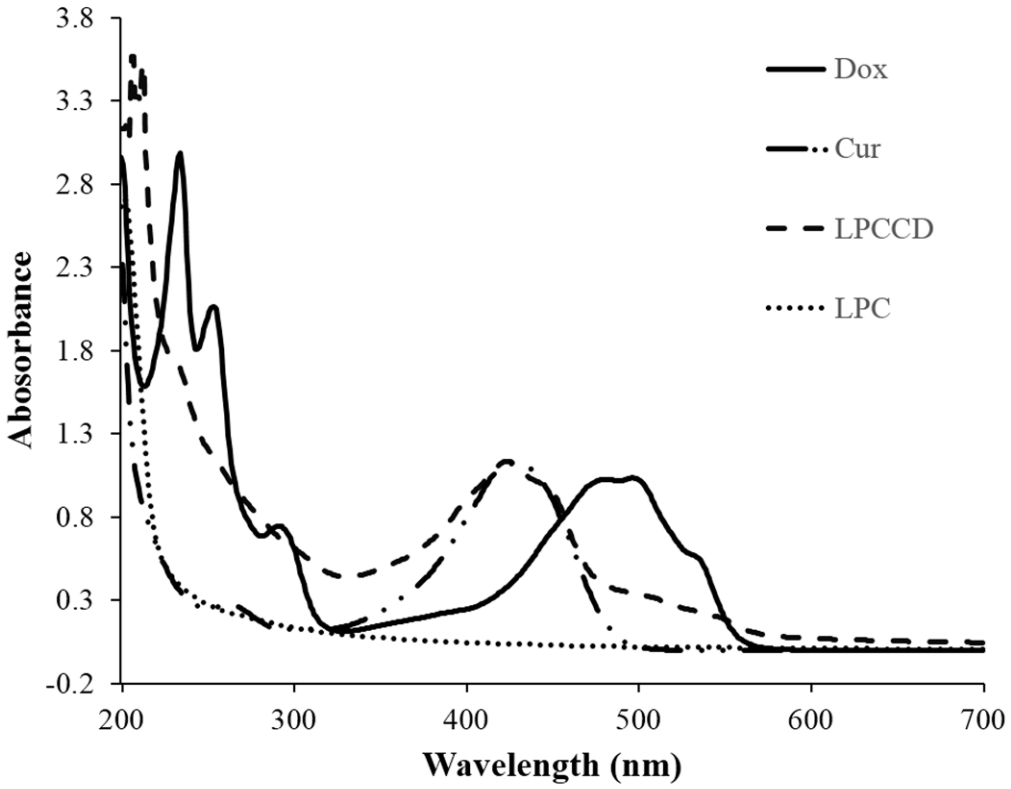

Fig. 4 UV spectrum of Dox, Cur, LPC and LPCCD.

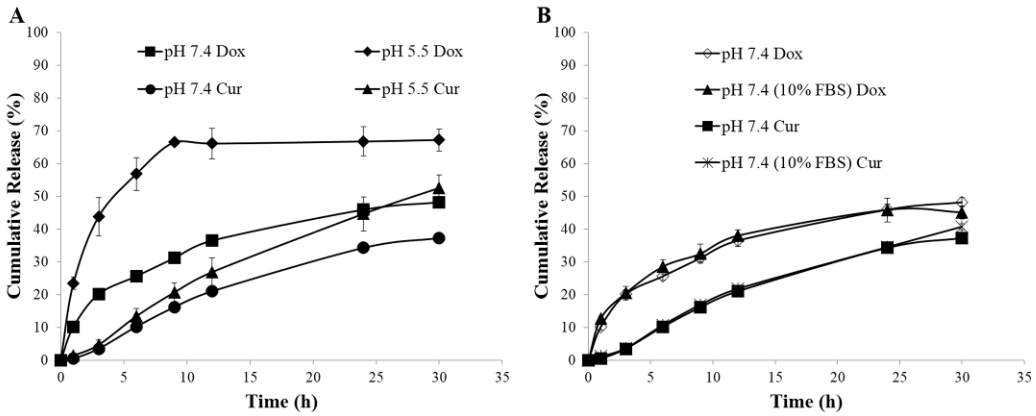

Fig. 5 Drug release behaviour of LPCCD. (A) pH-sensitive drug release of LPCCD in 0.01 M pH 7.4 Hepes buffer (including 0.1% Tween 80) and 0.01 M pH 5.5 Mes buffer (including 0.1% Tween 80). (B) LPCCD alone or mixed with 10% FBS in 0.01 M pH 7.4 Hepes buffer (including 0.1% Tween 80). Each point represents the mean ± S.D. of three experiments.

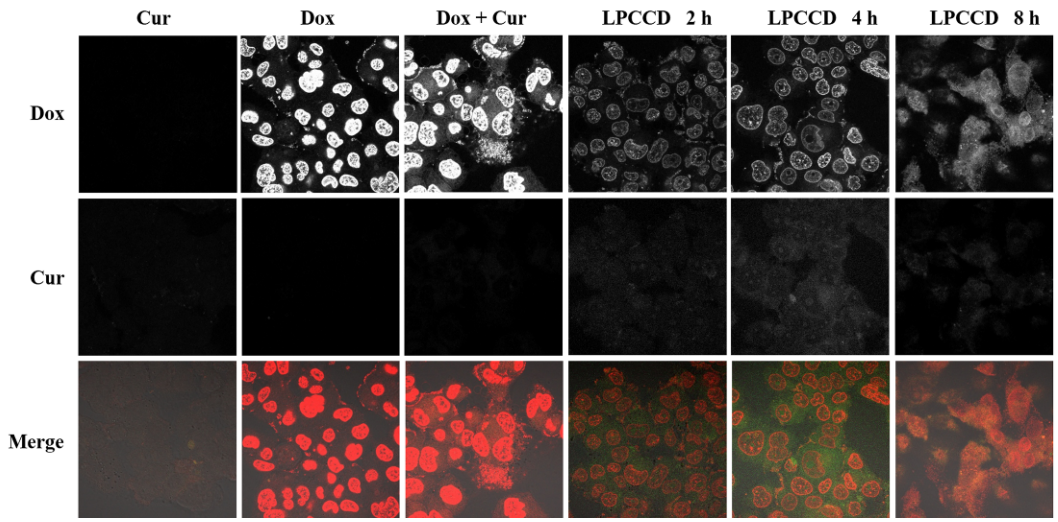

Fig. 6 Cellular uptake of free Cur, free Dox and free Dox + Cur at 2 h, and LPCCD at 2, 4 and 8 h, observed using confocal microscopy (at an equivalent concentration of Dox of 10 μM).

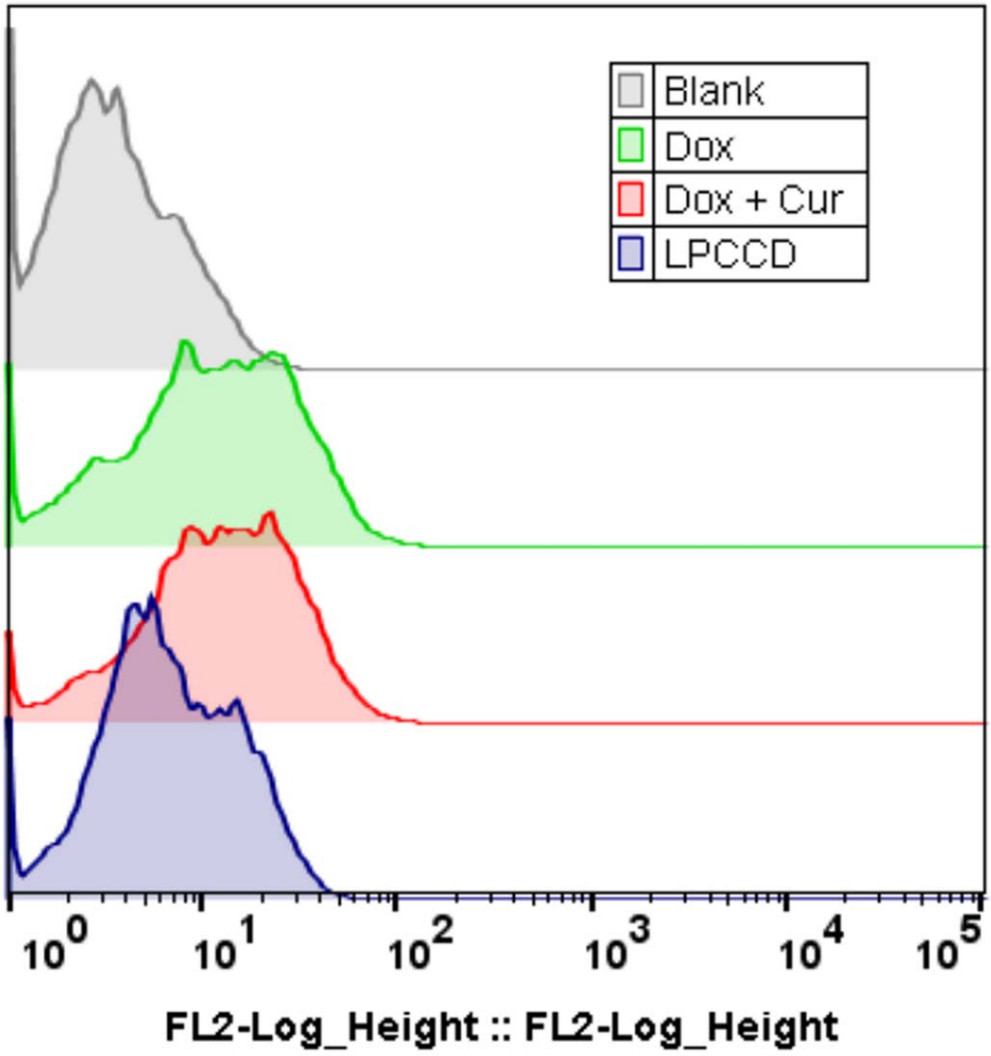

Group	Blank	Dox	Dox+Cur	LPCCD
MFI	4.35	16.2	16.9	9.03

Fig. 7 Cellular uptake of free Dox, free Dox + Cur and LPCCD at 4 h, as detected using a flow cytometer (at an equivalent concentration of Dox of 10 μM).

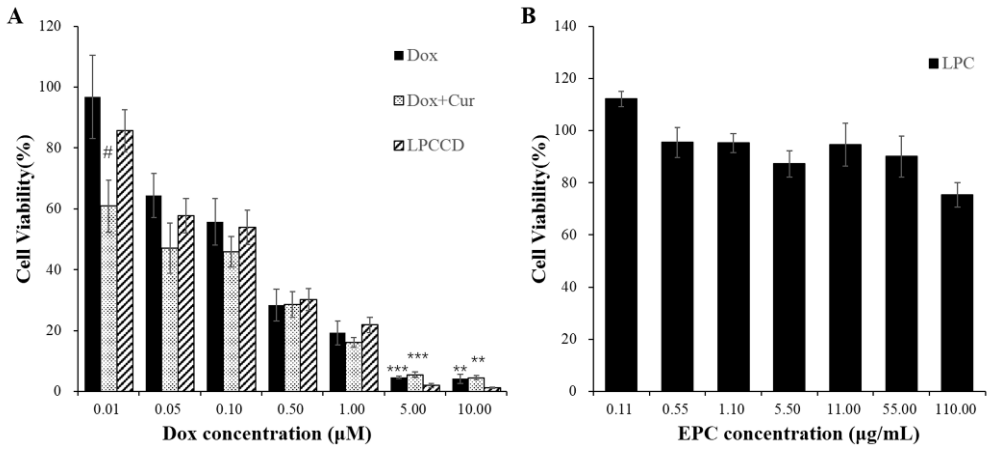

Fig. 8 Cytotoxicity of (A) free Dox, free Dox + Cur, LPCCD and (B) LPC, as detected using Cell counting kit-8. Each point represents the mean ± SD of three experiments. Significant differences from LPCCD and free Dox group are represented as $^{**}p<0.01$, $^{***}p<0.001$ and $^{\#}p<0.05$, respectively.

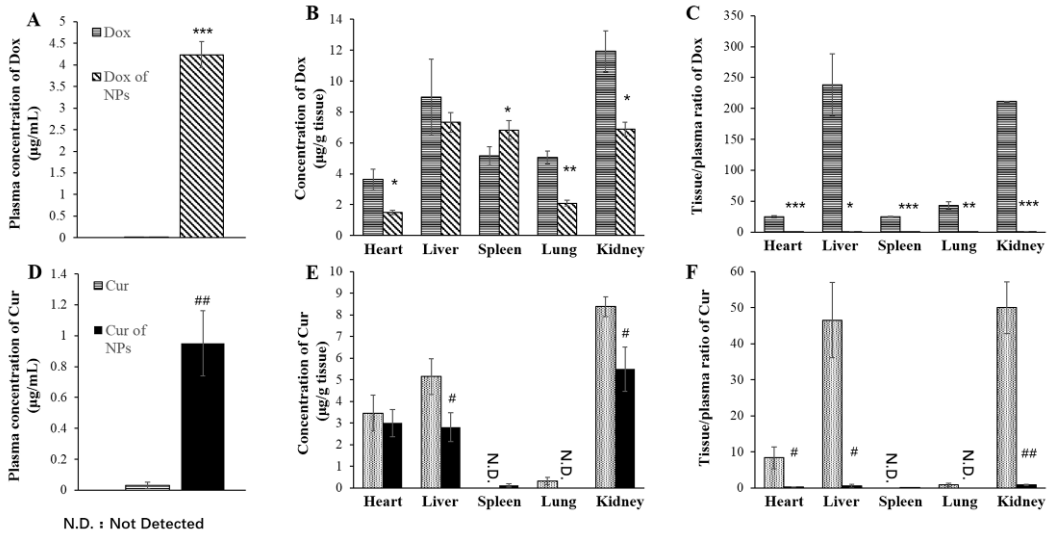

Fig. 9 Bio-distribution of doxorubicin (Dox) and curcumin (Cur) after intravenous administration of free Dox + Cur and LPCCD in mice. (A, D) Plasma concentration. (B, E) Accumulation in tissues. (C, F) Tissue/plasma ratio. Each bar represents the mean ± SD of three experiments. Significant differences from the free Dox + Cur group are represented as *p<0.05, **p<0.01, ***p<0.001 for Dox and $^{\#}p$<0.05, $^{\#\#}p$<0.01 for Cur. N.D., not detected.

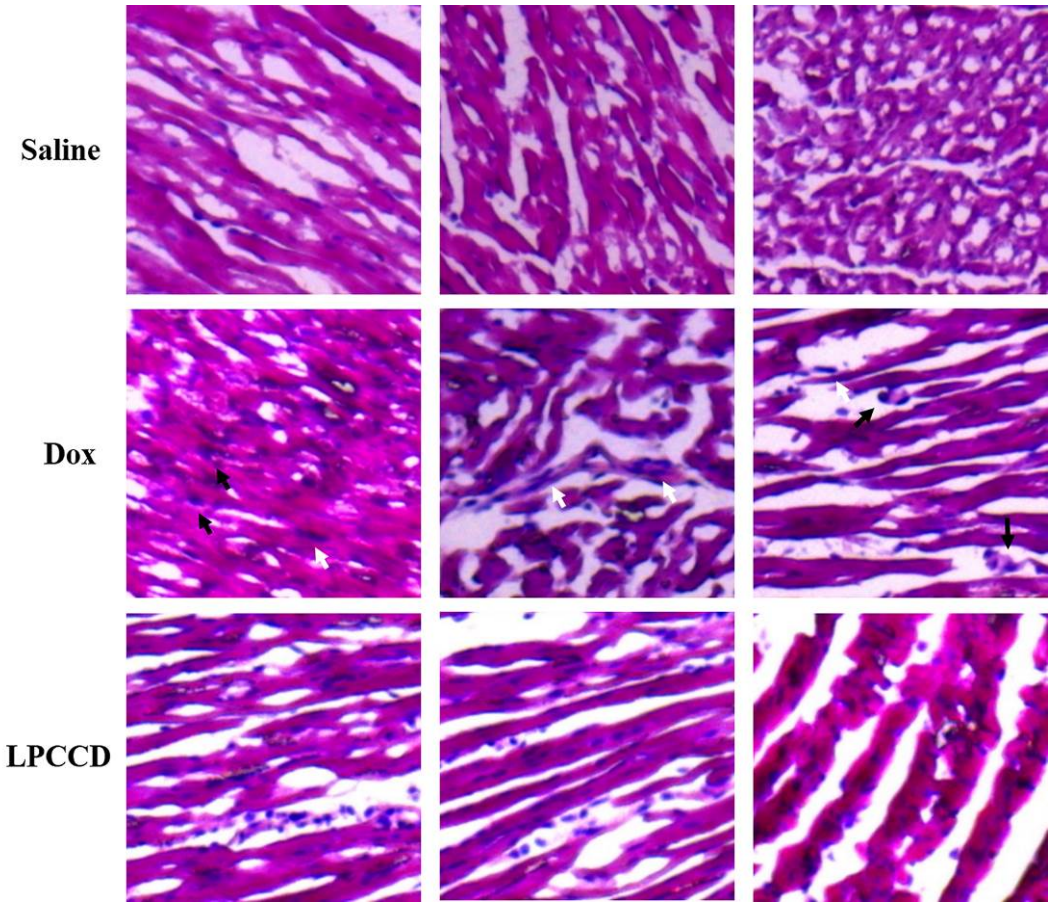

Fig. 10 Histopathological study of cardiotoxicity in mice treated with saline, free Dox and LPCCD. The presence of hypertrophic cardiac cells is indicated by white arrows and significant oedema is indicated by black arrows.

Journal of Drug Targeting

Supplementary figures

One-step formation of lipid-polyacrylic acid-calcium carbonate nanoparticles for co-delivery of doxorubicin and curcumin

Jianqing Peng [a], Shintaro Fumoto [a,*], Hirotaka Miyamoto [a], Yi Chen [b], Naotaka Kuroda [a], Koyo Nishida [a]

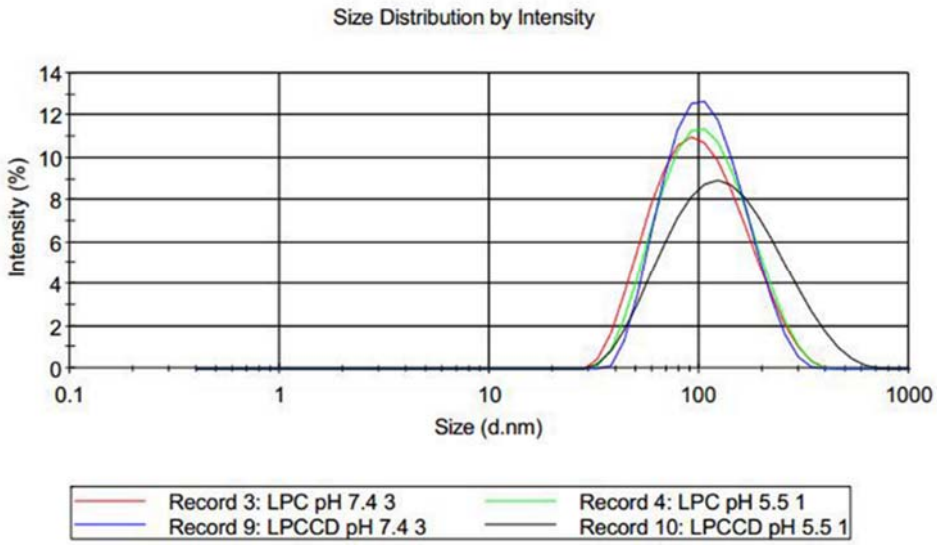

Supplementary Fig. 1 Particle size distributions of LPC and LPCCD in 0.01 M pH 7.4 Hepes buffer and 0.01 M pH 5.5 Mes buffer.

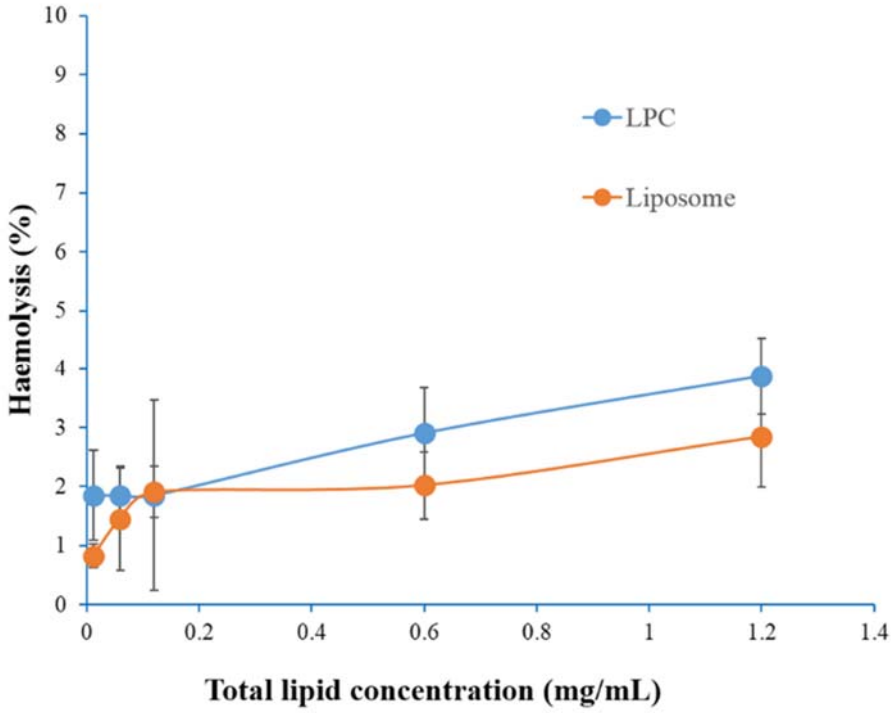

Supplementary Fig. 2 Haemolysis activity of liposomes (prepared without drugs, PAA and $CaCO_3$) and LPC at different total lipid concentrations.